Influence functionals with semiclassical propagators in combined forward–backward time

Keiran Thompson and Nancy Makri[a)]
School of Chemical Sciences, University of Illinois, 601 South Goodwin Avenue, Urbana, Illinois 61801

(Received 10 July 1998; accepted 24 September 1998)

In a recent letter [Chem. Phys. Lett. **291**, 101 (1998)] we presented a semiclassical methodology for calculating influence functionals arising from many-body anharmonic environments in the path integral formulation of quantum dynamics. Taking advantage of the trace operation associated with the unobservable medium, we express the influence functional in terms of a single propagator along a combined forward–backward system path. This propagator is evaluated according to time-dependent semiclassical theory in a coherent state initial value representation. Because the action associated with propagation in combined forward and backward time is governed by the *net* force experienced by the environment due to its interaction with the system, the resulting propagator is generally a smooth function of coordinates and thus amenable to Monte Carlo sampling; yet, the interference between forward and reverse propagators is fully accounted for. In the present paper we present a more elaborate version of the semiclassical influence functional formalism, along with algorithms for evaluating the coherent state transform of the Boltzmann operator that enters the influence functional. This factor is evaluated by performing an imaginary time path integral, and various approximations of the resulting expression as well as sampling schemes are discussed. The feasibility of the approach is demonstrated via numerous test calculations involving a two-level system coupled to (a) a dissipative harmonic bath and (b) a ten-dimensional bath of coupled anharmonic oscillators. © *1999 American Institute of Physics.* [S0021-9606(99)01301-X]

I. INTRODUCTION

The simulation of dynamical processes in molecular or condensed phase systems via *ab initio* quantum mechanics methods appears to require numerical effort that grows exponentially with the number of coupled degrees of freedom. While direct solution of the (stationary or time-dependent) Schrödinger equation necessitates the storage of multidimensional wave functions and manipulation of large matrices, the alternative path integral approach requires evaluation of high-dimensional integrals which is plagued by the ubiquitous phase cancellation problem. Although progress can be made in certain situations involving sparse matrix methods for intramolecular energy transfer[1,2] or inversion of imaginary time quantities[3,4] and in the simulation of processes in dissipative harmonic media,[5–11] rigorous real-time calculations on anharmonic many-particle systems remain out of reach.

Rather than targeting the polyatomic system as a whole, considerable attention has been given to methods combining a quantum mechanical description of the particle of interest with classical trajectory treatments of its surrounding atoms, which experience an Ehrenfest force (see, for example, Ref. 12). Recent studies on model systems have shown[13] that mixed quantum-classical schemes often lead to reasonable (though not quantitative) results, while their feasibility for describing polyatomic processes governed by anharmonic potentials is not known. A unified semiclassical description of all degrees of freedom in the spirit of the Van Vleck propagator is extremely appealing but suffers in practice from phase cancellation problems similar to those encountered in the fully quantum path integral description. This barrier is partly overcome by filtering techniques[14,15] and also in a linearized approximation to the semiclassical expression for flux correlation functions obtained recently by Miller and co-workers[13] which appears very promising.

In a recent article[16] we introduced a rigorous quantum-semiclassical approach which employs a path integral representation of the propagator for the observable particle along with a semiclassical Van Vleck treatment of the environment whose effects on the dynamics of interest enter via an influence functional. Since both system and solvent are described via appropriate propagators, the quantum-semiclassical description is equivalent to taking the $\hbar \to 0$ limit with respect to the bath, introducing no dynamical approximations. From the practical standpoint a fully semiclassical treatment of the solvent appears computationally prohibitive, since it entails a many-body calculation in itself. However, the definition of the bath as the collection of degrees of freedom which are not directly observable in a particular experiment gives rise to an ensemble average of a time evolution operator for the bath along a forward–backward system path; evaluating the latter via trajectories that evolve forward and backward in time gives rise to expressions where the troublesome interference between propagators is fully accounted for. The remaining phase cancellation associated with performing the ensemble average is minimal for statistically significant system paths, making Monte Carlo integration feasible.

Section II describes the formalism in detail, introducing the coherent state initial value representation of the semiclassical propagator and the expression of the influence functional in terms of forward–backward trajectories. Evaluation

a)Electronic mail: nancy@makri.scs.uiuc.edu

of the obtained expression requires knowledge of the coherent state transform of the canonical density operator, and this issue is addressed in Sec. III via approximate high temperature expressions or an imaginary time path integral treatment. Section IV describes Monte Carlo schemes for evaluating the semiclassical influence functional. Numerical examples presented in Sec. V illustrate the advantages and the convergence characteristics of the present formulation. Finally, Sec. VI presents some concluding remarks.

II. PATH INTEGRAL AND SEMICLASSICAL INFLUENCE FUNCTIONAL

Our goal is to devise a rigorous methodology suitable for following the dynamics of a quantum particle (the ''solute'') in a nearly classical environment of several interacting degrees of freedom which constitute the ''bath.'' The overall Hamiltonian is decomposed into system and bath terms as follows:

$$H(s,p_s,q,p)\equiv H_0(s,p_s)+H_{\rm env}(s,q,p). \tag{2.1a}$$

Here s denotes the coordinate(s) of the quantum system of interest and

$$H_{\rm env}(s,q,p)\equiv H_b(q,p)+V_{\rm int}(s,q) \tag{2.1b}$$

is the Hamiltonian for the unobservable environment (the bath) and its interaction with the system. For simplicity of presentation we use one-dimensional notation for the environment, although the treatment presented in this paper is intended primarily for a multidimensional bath. It is assumed that the coupling term involves only position operators.

A. Path integral representation of the reduced density matrix

For concreteness we focus on the reduced density matrix of the system, defined as

$$\tilde{\rho}(s',s'';t)\equiv {\rm Tr}_b\langle s'|e^{-iHt/\hbar}\rho(0)e^{iHt/\hbar}|s''\rangle, \tag{2.2}$$

where $\rho(0)$ is the initial density operator of the composite Hamiltonian and the trace is evaluated with respect to the bath. In the present paper we assume that the bath is initially at thermal equilibrium and is independent of the system, such that the initial density operator factorizes:

$$\rho(0)=\tilde{\rho}(0)e^{-\beta H_b}. \tag{2.3}$$

The extension to deal with nonseparable initial conditions is straightforward and has been discussed briefly in Ref. 13. Using the path integral representation[17] of the time evolution operators, Eq. (2.2) is brought into the form

$$\begin{aligned}\tilde{\rho}(s',s'';t)\equiv &\int ds_0^+\int ds_0^-\int \mathcal{D}s^+\int \mathcal{D}s^-\\ &\times\exp(iS_0[s^+]/\hbar)\tilde{\rho}(s_0^+,s_0^-;0)\\ &\times\exp(-iS_0[s^-]/\hbar)F[s^+,s^-].\end{aligned} \tag{2.4}$$

Here s^+ and s^- are system paths with endpoints (s_0^+,s') and (s_0^-,s'') for the forward and backward time evolution operators, respectively, and S_0 is the action for the system Hamiltonian H_0. Finally, F is the influence functional[17] of the bath, which can be written in the form

$$\begin{aligned}F[s^+,s^-]&=Q_b^{-1}\,{\rm Tr}_b[\hat{T}\exp(-iH_{\rm env}[s^+]t/\hbar)\\ &\quad\times\exp(-\beta H_b)\hat{T}^{-1}\exp(iH_{\rm env}[s^-]t/\hbar)]\\ &\equiv Q_b^{-1}\,{\rm Tr}_b[U_{\rm env}[s^+]\exp(-\beta H_b)\,U_{\rm env}^{-1}[s^-]].\end{aligned} \tag{2.5}$$

In the last equation $\hat{T}$ is the time ordering operator and

$$Q_b={\rm Tr}_b\,e^{-\beta H_b} \tag{2.6}$$

is the quantum partition function of the isolated medium. A simple rearrangement brings Eq. (2.6) into the form

$$F[s_+,s_-]=Q_b^{-1}\,{\rm Tr}_b(U_{\rm env}^{-1}[s_-]U_{\rm env}[s_+]e^{-\beta H_b}). \tag{2.7}$$

Similar expressions can be obtained for correlation functions of operators that pertain only to the observable system.

Since our goal is the development of a numerical method for obtaining the reduced density matrix we present below the discretized path integral representation of Eqs. (2.4)–(2.7). Splitting the total time t into N time slices of length $\Delta t=t/N$ and inserting complete sets of system position states leads to the expression:

$$\begin{aligned}\tilde{\rho}(s_N^+,s_N^-;t)\equiv {\rm Tr}_b&\int ds_0^+\int ds_1^+\cdots\int ds_{N-1}^+\int ds_0^-\\ &\times\int ds_1^-\cdots\int ds_{N-1}^-\langle s_N^+|e^{-iH\Delta t/\hbar}|s_{N-1}^+\rangle\\ &\times\langle s_{N-1}^+|e^{-iH\Delta t/\hbar}|s_{N-2}^+\rangle\cdots\langle s_1^+|e^{-iH\Delta t/\hbar}|s_0^+\rangle\\ &\times\langle s_0^+|\rho(0)|s_0^-\rangle\langle s_0^-|e^{iH\Delta t/\hbar}|s_1^-\rangle\cdots\\ &\times\langle s_{N-1}^-|e^{iH\Delta t/\hbar}|s_N^-\rangle,\end{aligned} \tag{2.8}$$

where for notational simplicity the reduced density matrix has been evaluated at the path endpoints $s_N^{\pm}$. Note that each propagator in the above equation is still an operator in the space of the bath. To obtain the discretized path integral representation of the reduced density matrix,[18] we split symmetrically the short time propagators into system and bath components:

$$e^{-iH\Delta t/\hbar}\approx e^{-iH_{\rm env}\Delta t/2\hbar}e^{-iH_0\Delta t/\hbar}e^{-iH_{\rm env}\Delta t/2\hbar}. \tag{2.9}$$

Using the last factorization and noting that the bath Hamiltonian depends only parametrically on the system, one obtains the following path integral representation of the reduced density matrix:

$$\tilde{\rho}(s_N^+,s_N^-;t)\equiv\int ds_0^+\int ds_1^+\cdots\int ds_{N-1}^+\int ds_0^-\int ds_1^-\cdots\int ds_{N-1}^-\langle s_N^+|e^{-iH_0\Delta t/\hbar}|s_{N-1}^+\rangle$$
$$\times\langle s_{N-1}^+|e^{-iH_0\Delta t/\hbar}|s_{N-2}^+\rangle\cdots\langle s_1^+|e^{-iH_0\Delta t/\hbar}|s_0^+\rangle\langle s_0^+|\tilde{\rho}(0)|s_0^-\rangle\langle s_0^-|e^{iH_0\Delta t/\hbar}|s_1^-\rangle\cdots\langle s_{N-1}^-|e^{iH_0\Delta t/\hbar}|s_N^-\rangle$$
$$\times F(s_0^\pm,s_1^\pm,\ldots,s_N^\pm;t). \tag{2.10}$$

Here F is the influence functional of the bath for a particular pair of linearized system forward and backward paths which, after a rearrangement of the operators, takes the form

$$F(s_0^\pm,s_1^\pm,\ldots,s_N^\pm;t)=Q_b^{-1}\,\mathrm{Tr}_b\left\{\exp\left(\frac{i}{\hbar}\frac{\Delta t}{2}H_{\mathrm{env}}(s_0^-)\right)\exp\left(\frac{i}{\hbar}\Delta t H_{\mathrm{env}}(s_1^-)\right)\cdots\exp\left(\frac{i}{\hbar}\frac{\Delta t}{2}H_{\mathrm{env}}(s_N^-)\right)\right.$$
$$\left.\times\exp\left(-\frac{i}{\hbar}\frac{\Delta t}{2}H_{\mathrm{env}}(s_N^+)\right)\cdots\exp\left(-\frac{i}{\hbar}\Delta t H_{\mathrm{env}}(s_1^+)\right)\exp\left(-\frac{i}{\hbar}\frac{\Delta t}{2}H_{\mathrm{env}}(s_0^+)\right)e^{-\beta H_b}\right\}. \tag{2.11}$$

B. Semiclassical representation of the influence functional

Evaluating the trace and inserting the identity operator brings Eq. (2.7) into the form

$$F[s_+,s_-]=Q_b^{-1}\int dq_0\int dq\langle q|U_{\mathrm{env}}^{-1}[s^-]U_{\mathrm{env}}[s^+]|q_0\rangle$$
$$\times\langle q_0|e^{-\beta H_b}|q\rangle. \tag{2.12}$$

It is convenient to view the real-time factor of the integrand in the above expression as a single time evolution operator along the time contour displayed in Fig. 1. As time increments from zero to t the bath evolves according to the Hamiltonian $H_{\mathrm{env}}(q,p,s^+(t'))$ which is time dependent by virtue of the coupling to the time dependent forward system path. Subsequently, the time returns to zero as the bath follows $H_{\mathrm{env}}[q,p,s^-(t')]$.

The goal is to evaluate the Boltzmann factor entering Eq. (2.12) quantum mechanically or via an acceptable approximation and to use the semiclassical expression for the real-time component. To this end we convert Eq. (2.12) to an initial value representation.[19–22] Noting that Eq. (2.12) can be rewritten formally in the form of a sum over bath eigenstates Φ_n with eigenvalues E_n,

$$F[s_+,s_-]=Q_b^{-1}\int dq_0\sum_{n=0}^{\infty}e^{-\beta E_n}\langle\Phi_n|q_0\rangle$$
$$\times\langle q_0|U_{\mathrm{env}}^{-1}[s_-]U_{\mathrm{env}}[s_+]|\Phi_n\rangle \tag{2.13}$$

and using the semiclassical coherent state representation of Herman and Kluk[23] for each basis function the influence functional becomes

$$F[s_+,s_-]=Q_b^{-1}(2\pi\hbar)^{-1}\sum_{n=0}^{\infty}e^{-\beta E_n}$$
$$\times\int dq_0\int dp_0\langle\Phi_n|G(q_f,p_f)\rangle D(q_0,p_0)$$
$$\times\exp\left(\frac{i}{\hbar}S_{\mathrm{env}}(q_0,p_0)\right)\langle G(q_0,p_0)|\Phi_n\rangle. \tag{2.14}$$

Here q_f and p_f are the final coordinate and momentum for a classical trajectory with initial conditions q_0,p_0 which evolves under the action of the combined forward–backward time evolution operators that appear in Eq. (2.12), S_{env} is the corresponding action, and D is the coherent state analog of the Van Vleck derivative, given by the expression[24]

$$D=\frac{1}{\sqrt{2}}\left(\frac{\partial q_f}{\partial q_0}+\frac{\partial p_f}{\partial p_0}-2i\hbar\gamma\frac{\partial q_f}{\partial p_0}+\frac{i}{2\hbar\gamma}\frac{\partial p_f}{\partial q_0}\right)^{\frac{1}{2}}. \tag{2.15}$$

Finally,

$$\langle q|G(q_0,p_0)\rangle=\left(\frac{2\gamma}{\pi}\right)^{1/4}\exp\left(-\gamma(q-q_0)^2+\frac{i}{\hbar}p_0(q-q_0)\right) \tag{2.16}$$

is a coherent state of momentum p_0 centered about q_0. The width parameter γ is at this stage completely arbitrary.

The classical trajectories entering Eq. (2.14) obey Hamilton's equations

$$\dot{q}(t)=\frac{\partial H_{\mathrm{env}}(t)}{\partial p},\quad \dot{p}(t)=-\frac{\partial H_{\mathrm{env}}(t)}{\partial q} \tag{2.17}$$

in the time-dependent bath Hamiltonian defined as

$$H_{\mathrm{env}}(t')=\begin{cases}H_{\mathrm{env}}(q,p,s_+(t')), & t'\uparrow\\ H_{\mathrm{env}}(q,p,s_-(t')), & t'\downarrow\end{cases} \tag{2.18}$$

and the action is given by

$$S_{\mathrm{env}}(q_0,p_0)=\int_0^t[p(t')\dot{q}(t')-H_{\mathrm{env}}(t')]dt'$$
$$+\int_t^0[p(t')\dot{q}(t')-H_{\mathrm{env}}(t')]dt'. \tag{2.19}$$

It is useful to note that all four terms entering Eq. (2.15) are elements of the stability matrix. Rearranging Eq. (2.14) and removing the bath eigenstates leads to the result

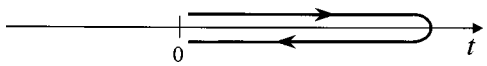

FIG. 1. Schematic representation of the time contour along which Eq. (2.20) is evaluated.

$$F[s_+,s_-]=Q_b^{-1}(2\pi\hbar)^{-1}\int dq_0\int dp_0 D(q_0,p_0)\times\exp\left(\frac{i}{\hbar}S_{\rm env}(q_0,p_0)\right)\times\langle G(q_0,p_0)|e^{-\beta H_b}|G(q_f,p_f)\rangle. \quad (2.20)$$

Equation (2.20) is the central result of Ref. 16. As will become clear below, this expression is in general amenable to Monte Carlo evaluation. Although the integrand of Eq. (2.14) is not strictly positive, the dominant terms in the action arising from the dynamics of the isolated bath (which are responsible for the highly oscillatory nature of the semiclassical propagator) *cancel* because of the backward propagation. Most importantly, one can show that the oscillations are mild for statistically significant system paths. Indeed, if the forward and backward paths coincide, each trajectory simply retraces its steps during the second part of the time contour and returns to its initial phase space location, while the total action integral equals zero.

III. COHERENT STATE BOLTZMANN FACTOR

To complete the prescription for evaluating the influence functional one needs an expression for the coherent state transform of the Boltzmann operator appearing in Eq. (2.14). Below we discuss various means of obtaining the latter.

A. High temperature

Using the Trotter splitting of the Boltzmann operator, the coherent state matrix element takes the form

$$\langle G(q_0,p_0)|e^{-\beta H_b}|G(q_f,p_f)\rangle \approx\int dq\langle G(q_0,p_0)|e^{-\beta T_b/2}|q\rangle\times e^{-\beta V_b(q)}\langle q|e^{-\beta T_b/2}|G(q_f,p_f)\rangle, \quad (3.1)$$

where T_b is the bath kinetic energy operator and V_b is the potential for the isolated bath. The kinetic energy factors in Eq. (3.1) can be found to be[16]

$$\langle G(q_0,p_0)|e^{-\beta T_b/2}|q_1\rangle =\left(\frac{2\gamma}{\pi}\right)^{\frac{1}{4}}\left(\frac{m}{m+\hbar^2\beta\gamma}\right)^{\frac{1}{2}}\times\exp\left[-\frac{m}{m+\hbar^2\beta\gamma}\left(\gamma(q_1-q_0)^2+\frac{\beta}{4m}p_0^2+\frac{i}{\hbar}p_0(q_1-q_0)\right)\right] \quad (3.2)$$

leading to the expression

$$\langle G(q_0,p_0)|e^{-\beta H_b}|G(q_f,p_f)\rangle \approx\sqrt{\frac{2\gamma}{\pi}}\frac{m}{\hbar^2\beta\gamma+m}\int dq\exp\left[-\frac{m}{\hbar^2\beta\gamma+m}\times\left(\gamma(q-q_0)^2+\gamma(q-q_f)^2+\frac{\beta}{4m}(p_0^2+p_f^2)+\frac{i}{\hbar}(p_0-p_f)q-\frac{i}{\hbar}(p_0q_0-p_fq_f)\right)-\beta V_b(q)\right]. \quad (3.3)$$

In general, full evaluation of Eq. (3.3) requires numerical integration. However, it is intriguing that the required integration in Eq. (3.2) can be approximated analytically in the spirit of the steepest decent method. If the coherent state parameter γ is sufficiently large the Gaussian factor in the above equation decays much faster than the high-temperature potential part. Further, if $\gamma\to\infty$ one can approximate the integral by adding the contributions of the integrand at the steepest descent points q_0 and q_f. On the other hand, if $\gamma^{-1/2}\gg|q_0-q_f|$ the two Gaussians overlap almost completely and it is advantageous to expand the integrand about the midpoint $\frac{1}{2}(q_0+q_f)$, leading to the result

$$\langle G(q_0,p_0)|e^{-\beta H_b}|G(q_f,p_f)\rangle \approx\sqrt{\frac{m}{\hbar^2\beta\gamma+m}}\exp\left[-\frac{m}{\hbar^2\beta\gamma+m}\left(\frac{\beta}{4m}(p_0^2+p_f^2)+\frac{i}{\hbar}(p_0+p_f)\frac{q_0-q_f}{2}\right)-\beta V_b\left(\frac{q_0+q_f}{2}\right)\right]. \quad (3.4)$$

Note that although the above approximate evaluations follow the idea of the steepest descent method, the quadratic nature of the rapidly decaying terms ensures uniqueness of the roots and the results can become arbitrarily accurate by choosing the coherent state parameter in the appropriate range.

B. Low temperature

At low temperatures application of the Trotter splitting to the entire Boltzmann operator is not a good approximation. We thus treat the low temperature case by performing a path integral in imaginary time.[18] Defining the imaginary time step $\Delta\beta\equiv\beta/n$, where n is an integer, expressing the coherent state Boltzmann factor as a path integral in terms of ordinary coordinate states and using Eq. (3.2) one arrives at the following path integral representation:

$$\langle G(q_0,p_0)|e^{-\beta H_b}|G(q_f,p_f)\rangle =\left(\frac{2\gamma}{\pi}\right)^{\frac{1}{2}}\left(\frac{m}{m+\hbar^2\Delta\beta\gamma}\right)\left(\frac{m}{2\pi\hbar^2\Delta\beta}\right)^{\frac{n-1}{2}}\int dq_1\cdots\int dq_n\times\exp\left[-\frac{m}{m+\hbar^2\Delta\beta\gamma}\left(\gamma(q_1-q_0)^2+\gamma(q_n-q_f)^2+\frac{\Delta\beta}{4m}(p_0^2+p_f^2)+\frac{i}{\hbar}p_0(q_1-q_0)-\frac{i}{\hbar}p_f(q_n-q_f)\right)-\frac{m}{2\hbar^2\Delta\beta}\sum_{k=2}^{n}(q_k-q_{k-1})^2-\Delta\beta\sum_{k=1}^{n}V_b(q_k)\right]. \quad (3.5)$$

This expression involves an n-dimensional integral for every bath mode. Combined with the phase space integrals of Eq. (2.20), the influence functional requires evaluation of an $(n+2)$-dimensional integral for each bath degree of freedom.

IV. MONTE CARLO PROCEDURES

In this section we describe Monte Carlo procedures for the numerical evaluation of the integrals required to evaluate the influence functional in the cases of high and low temperature.

A. High temperature

With the high temperature approximation of the coherent state Boltzmann operator obtained in Sec. III A, the semiclassical influence functional becomes

$$F[s_+,s_-] = (2\pi\hbar)^{-1}\sqrt{\frac{2\gamma}{\pi}}\frac{m}{\hbar^2\beta\gamma+m}Q_b^{-1}\int dq_0\int dp_0\int dq \times\exp\Bigg[-\frac{m}{\hbar^2\beta\gamma+m}\Big(\gamma(q-q_0)^2+\gamma(q-q_f)^2 + \frac{\beta}{4m}(p_0^2+p_f^2)+\frac{i}{\hbar}(p_0-p_f)q-\frac{i}{\hbar}(p_0q_0-p_fq_f)\Big), -\beta V_b(q)+\frac{i}{\hbar}S_{\rm env}(q_0,p_0)\Bigg]. \tag{4.1}$$

It is convenient to employ a sampling function r that depends on the bath trajectories only through their initial conditions:

$$r(q_0,p_0,q) = \exp\Bigg[-\frac{m}{\hbar^2\beta\gamma+m}\Big(\gamma(q-q_0)^2+\frac{\beta}{4m}p_0^2\Big)-\beta V_b(q)\Bigg]. \tag{4.2}$$

Performing the phase space integrals analytically and noting that the integral over q is proportional to the partition function in the high-temperature approximation, one obtains the following expression for the normalization integral of the sampling function:

$$\int dq_0\int dp_0\int dq\; r(q_0,p_0,q) = 2\pi\frac{m+\hbar^2\beta\gamma}{\sqrt{m\beta\gamma}}\sqrt{\frac{2\pi\hbar^2\beta}{m}}Q_b. \tag{4.3}$$

Multiplying Eq. (4.1) by the normalization integral and changing the q_0 integration variable to $y\equiv q_0-q$ in order to facilitate sampling leads to the final result for the influence functional of a high-temperature bath:

$$F[s^+,s^-] = 2\int dp_0\int dq\int d(q_0-q)\,r_{\rm norm}(q_0,p_0,q) \times\exp\Bigg[-\frac{m}{\hbar^2\beta\gamma+m}\Big(\gamma(q-q_f)^2+\frac{\beta}{4m}p_f^2 + \frac{i}{\hbar}(p_0-p_f)q-\frac{i}{\hbar}(p_0q_0-p_fq_f)\Big) + \frac{i}{\hbar}S_{\rm env}(q_0,p_0)\Bigg] \tag{4.4}$$

where $r_{\rm norm}$ is a *normalized* sampling function proportional to Eq. (4.2).

B. Low temperature

Inserting the imaginary time path integral expression for the coherent state matrix elements of the Boltzmann operator, obtained in Sec. III B, into Eq. (2.20) the semiclassical influence functional becomes

$$F[s^+,s^-] = Q_b^{-1}(2\pi\hbar)^{-1}\Big(\frac{2\gamma}{\pi}\Big)^{1/2}\Big(\frac{m}{m+\hbar^2\Delta\beta\gamma}\Big)\Big(\frac{m}{2\pi\hbar^2\Delta\beta}\Big)^{\frac{n-1}{2}}\int dq_0\int dp_0\int dq_1\ldots\int dq_n \times D(q_0,p_0)\exp\Big(\frac{i}{\hbar}S_{\rm env}(q_0,p_0)\Big)\exp\Bigg[\frac{m}{m+\hbar^2\Delta\beta\gamma}\Big(\gamma(q_1-q_0)^2+\gamma(q_n-q_f)^2 + \frac{\Delta\beta}{4m}(p_0^2+p_f^2)+\frac{i}{\hbar}p_0(q_1-q_0)-\frac{i}{\hbar}p_f(q_n-q_f)\Big)-\frac{m}{2\hbar^2\Delta\beta}\sum_{k=2}^{n}(q_k-q_{k-1})^2-\Delta\beta\sum_{k=1}^{n}V_b(q_k)\Bigg]. \tag{4.5}$$

In order to minimize the oscillations in the integrand, one would like to arrange for the two imaginary terms in the exponent of Eq. (4.5) to cancel to as large an extent as possible. Clearly, it is advantageous to choose the coherent state parameter γ large, in order to make the real Gaussian in Eq. (4.5) as narrow as possible, while maximizing the oscillation wavelength of the imaginary components. Then, for similar system paths for which $q_f\approx q_0$ and $p_f\approx p_0$, the Gaussians ensure that $q_1\approx q_0$ and $q_n\approx q_f$, implying $q_1\approx q_n$. Under such conditions the complex part of the integrand nearly vanishes while the remaining small contribution will oscillate sufficiently slowly that it may not change sign within the effective integration range.

Now the choice of sampling function for Monte Carlo

integration is more subtle than in the high-temperature approximation of Sec. IV A. It is not possible to construct an easily normalizable sampling function for Eq. (4.5) which depends only on the trajectory initial conditions. Accordingly, we use a sampling function that is based on the linearized approximation to the trajectory,

$$q_f^L = q_0 - \frac{1}{m\omega_0}\int_0^t \Delta f(t')\sin\omega_0 t'\,dt' \equiv q_0 - b, \quad p_f^L = p_0, \tag{4.6}$$

where $\Delta f(t') = f[s^+(t')] - f[s^-(t')]$ is the net force experienced by the bath and ω_0 is the harmonic frequency at a reference configuration, and define the sampling function

$$\begin{aligned} r(q_0,p_0,q_1,\ldots,q_n) &= \exp\Bigg[-\frac{m}{m+\hbar^2\Delta\beta\gamma}\Bigg(\gamma(q_1-q_0)^2 + \gamma(q_n-q_f^L)^2 \\ &\quad + \frac{\Delta\beta}{4m}(p_0^2+p_f^{L^2})\Bigg) - \frac{m}{2\hbar^2\Delta\beta} \\ &\quad \times \sum_{k=2}^{n}(q_k-q_{k-1})^2 - \Delta\beta\sum_{k=1}^{n} V_b(q_k)\Bigg]. \end{aligned} \tag{4.7}$$

Performing the Gaussian integrals, the normalization integral of this function is found to be given by the expression

$$\begin{aligned} &\int dq_0 \int dp_0 \int dq_1 \cdots \int dq_n r(q_0,p_0,q_1,\ldots,q_n) \\ &= \pi \frac{m+\hbar^2\Delta\beta\gamma}{\sqrt{m\gamma\Delta\beta}} \int dq_1 \cdots \int dq_n \\ &\quad \times \exp\Bigg(-\frac{m\gamma/2}{m+\hbar^2\Delta\beta\gamma}(q_1-q_n-b)^2 \\ &\quad - \frac{m}{2\hbar^2\Delta\beta}\sum_{k=2}^{n}(q_k-q_{k-1})^2 - \Delta\beta\sum_{k=1}^{n} V_b(q_k)\Bigg). \end{aligned} \tag{4.8}$$

To calculate the last integral we define the normalized function

$$\begin{aligned} &f_{\mathrm{norm}}(q_1,\ldots,q_n) \\ &\quad \equiv \frac{1}{\mu}\exp\Bigg(-\frac{m}{2\hbar^2\Delta\beta}\sum_{k=2}^{n}(q_k-q_{k-1})^2 - \Delta\beta\sum_{k=1}^{n} V_b(q_k)\Bigg), \end{aligned} \tag{4.9a}$$

where

$$\begin{aligned} \mu \equiv \int dq_1 \cdots \int dq_n \exp\Bigg(&-\frac{m}{2\hbar^2\Delta\beta}\sum_{k=2}^{n}(q_k-q_{k-1})^2 \\ &- \Delta\beta\sum_{k=1}^{n} V_b(q_k)\Bigg). \end{aligned} \tag{4.9b}$$

The integral in Eq. (4.8) is easily obtained using f_{norm} as the sampling function:

$$\begin{aligned} \lambda &\equiv \mu^{-1}\int dq_1 \cdots \int dq_n \exp\Bigg(-\frac{m\gamma/2}{m+\hbar^2\Delta\beta\gamma}(q_1-q_n-b)^2 - \frac{m}{2\hbar^2\Delta\beta}\sum_{k=2}^{n}(q_k-q_{k-1})^2 - \Delta\beta\sum_{k=1}^{n} V(q_k)\Bigg) \\ &= \int dq_1 \cdots \int dq_n \exp\Bigg[-\frac{m}{m+\hbar^2\Delta\beta\gamma}\Bigg(\gamma q_1^2 + \gamma(q_n+b)^2 - \frac{\gamma}{2}(q_1+q_n+b)^2\Bigg)\Bigg] f_{\mathrm{norm}}(q_1,\ldots,q_n). \end{aligned} \tag{4.10}$$

Finally, notice that the partition function can also be obtained in terms of this function:

$$Q_b = \left(\frac{m}{2\pi\hbar^2\Delta\beta}\right)^{n/2}\int dq_1 \cdots \int dq_n \mu f_{\mathrm{norm}}(q_1,\ldots q_n)\exp\left(-\frac{m}{2\hbar^2\Delta\beta}(q_1-q_n)^2\right) = \left(\frac{m}{2\pi\hbar^2\Delta\beta}\right)^{n/2}\mu\kappa, \tag{4.11a}$$

where

$$\kappa \equiv \int dq_1 \cdots \int dq_n f_{\mathrm{norm}}(q_1,\ldots q_n)\exp\left(\frac{m}{2\hbar^2\Delta\beta}(q_1-q_n)^2\right). \tag{4.11b}$$

Combining these equations, one finds

$$Q_b^{-1}\int dq_0 \int dp_0 \int dq_1 \cdots \int dq_n r(q_0,p_0,q_1,\ldots,q_n) = \pi\frac{m+\hbar^2\Delta\beta\gamma}{\sqrt{m\gamma\Delta\beta}}(\lambda\,\mu)\left(\frac{m}{2\pi\hbar^2\Delta\beta}\right)^{-n/2}\mu^{-1}\kappa^{-1}. \tag{4.12}$$

Making use of Eq. (4.12), the influence functional expression given by Eq. (4.5) becomes

$$F[s_+,s_-]=\frac{\lambda}{\kappa}\int dq_0\int dp_0\int dq_1\ldots\int dq_n r_{\rm norm}(q_0,p_0,q_1,\ldots,q_n)D(q_0,p_0)$$
$$\times\exp\left(\frac{i}{\hbar}S_{\rm env}(q_0,p_0)\right)\exp\left[-\frac{m}{m+\hbar^2\Delta\beta\gamma}\left(2\gamma q_n(q_f^L-q_f)+\gamma(q_f^2-q_f^{L^2})^2\right.\right.$$
$$\left.\left.+\frac{i}{\hbar}p_0(q_1-q_0)-\frac{i}{\hbar}p_f(q_n-q_f)\right)\right], \tag{4.13}$$

where $r_{\rm norm}$ is again a normalized sampling function of $(n+2)$ variables for each bath degree of freedom, proportional to Eq. (4.7). Note that κ is a constant of the isolated bath, while λ must be reevaluated for each influence functional calculation. As their integrands are strictly positive and localized, both integrals are easily obtained by Monte Carlo with the normalized sampling function $f_{\rm norm}$.

V. ANALYTIC AND NUMERICAL EXAMPLES

This section examines the convergence characteristics of the methodology detailed in Secs. II–IV and its applicability to realistic multidimensional systems. We begin with the prototype of a harmonic oscillator bath, for which the various expressions can be evaluated analytically, illustrating a very desirable behavior achieved by combining forward and backward evolution. In an earlier paper we showed that the forward–backward semiclassical influence functional methodology can be applied to a harmonic bath at high temperature using a modest number of sampled trajectories. Here we present further results in various regimes at high temperature and demonstrate convergence of the imaginary time path integral formulation by application to a harmonic bath at low temperature. Finally, a simple model of a one-dimensional chain of atoms is used as a coupled anharmonic bath, demonstrating the generality of our approach.

A. Harmonic bath

We begin by summarizing the forward–backward influence functional expression for the one-dimensional harmonic bath considered in Ref. 16. The Hamiltonian has the form

$$H_b=\frac{p^2}{2m}+\frac{1}{2}m\omega^2q^2-csq. \tag{5.1}$$

Using the well-known forced harmonic oscillator algebra for the forward and backward branches, one finds

$$q_f=q_0-\frac{c}{m\omega}\int_0^t\Delta s(t')\sin\omega t'\,dt'$$

and

$$p_f=p_0+c\int_0^t\Delta s(t')\cos\omega t'\,dt', \tag{5.2}$$

where

$$\Delta s(t')\equiv s^+(t')-s^-(t'). \tag{5.3}$$

Evaluation of the forward–backward action yields the result

$$S(q_0,p_0)=cq_0\int_0^t\Delta s(t')\cos\omega t'\,dt'+c^2g[s_+,s_-], \tag{5.4}$$

where g depends on the forward and backward system paths alone. Notice that the quadratic terms present in the harmonic oscillator action for forward time evolution have been eliminated. Interestingly, the dependence on initial momentum has also disappeared as a consequence of linearity. As a result, the rapid oscillations in the semiclassical propagator are largely eliminated: no oscillations occur in p_0 and the oscillations in the q_0 variable are relatively mild as the action now depends on that variable only linearly with a prefactor that is proportional to the *net* force experienced by the bath. In the classical limit where the forward and backward paths are the same the action is independent of both integration variables. As illustrated graphically in Ref. 16, the propagator arising from Eq. (5.4) is much better suited to Monte Carlo integration.

Next, we test the ability of this methodology to describe dissipative dynamics by applying it to calculate the time evolution of the celebrated spin-boson Hamiltonian.[25] As before we consider the average value of position of a two-level system (TLS) coupled to a dissipative bath described by an ohmic spectral density with exponential cutoff:

$$J(\omega)=\tfrac{1}{2}\pi\hbar\xi\omega e^{-\omega/\omega_c}. \tag{5.5}$$

Here ξ is the so-called Kondo parameter, which is a measure of the overall system-bath coupling strength, and the cutoff frequency ω_c corresponds to the maximum of the spectral density. For the purpose of performing the semiclassical calculation the bath must be discretized. Using a procedure motivated by the theory of solids,[26] the discrete bath results converge to those of an infinite-dimensional bath with only ten bath oscillators. The total Hamiltonian is

$$H=-\hbar\Omega\sigma_x+\sum_j\left(\frac{p_j^2}{2m_j}+\frac{1}{2}m_j\omega_j^2q_j^2-c_j\sigma_zq_j\right), \tag{5.6}$$

where σ_x and σ_z are the usual Pauli spin matrices. The tunneling splitting of the isolated two-level system is equal to $2\hbar\Omega$. Below we present the results of the semiclassical procedure described in this paper and compare to those obtained via the exact Feynman–Vernon influence functional[27] for various combinations of temperature and system-bath coupling strength. In both cases, the path integral is evaluated via global summation over all TLS paths with up to five time slices. The cutoff frequency is chosen to be $\omega_c=3\ \Omega$.

TABLE I. Real part of select influence functionals for the harmonic bath model with $N=5$ at two values of the Kondo parameter. The Boltzmann factor is evaluated with $n=1$ or 4 imaginary time slices. Each entry lists the configuration of a forward/backward path combination of the times $\{0,1\ldots,N\}$. The symbols R and L denote right and left sites of the TLS. The temperature is $\hbar\omega_c\beta=3$.

	$\xi=0.1$			$\xi=0.5$		
TLS paths	$n=1$	$n=4$	Exact	$n=1$	$n=4$	Exact
RRLRLR RLLRLR	0.624±0.05	0.756±0.02	0.7922	0.083±0.02	0.216±0.02	0.2448
RRLLLR RLRLLR	0.753±0.05	0.828±0.03	0.8440	0.278±0.04	0.376±0.03	0.3480

In the calculations presented in this section the TLS is initially localized in the right state. Consequently, only the real part of each influence functional contributes to the average position. Table I shows the real part of the influence functional for a harmonic bath at a temperature of $\beta^{-1}=\frac{1}{3}\hbar\omega_c$ evaluated on illustrative forward–backward paths consisting of $N=5$ time slices. The uncertainties in the influence functional values arise from the Monte Carlo integration and represent 1 standard deviation (s.d.) from the mean. The results shown in Table I with $n=1$ and $n=4$ used 5000 and 10 000 Monte Carlo points per integration variable, respectively. The exact influence functionals were obtained from the Feynman–Vernon formulas for a continuous harmonic bath. For both high ($\xi=0.5$) and low ($\xi=0.1$) friction the high-temperature approximation ($n=1$ results) is inaccurate but the low temperature expression with four imaginary time slices produced results which are consistently within 2 s.d. of the exact values.

Path integral results for the TLS average position are shown in Figs. 2 and 3. Figure 2 presents numerical results for this system at a range of coupling strengths at a high temperature ($\hbar\omega_c\beta=0.05$). At this temperature the evolution of the TLS follows exponential decay. The high-temperature ($n=1$) expression for the semiclassical influence functional was evaluated using 5000 Monte Carlo points for each of the 3×10 integration variables in Eq. (4.4). Including an equilibration period of 15 000 steps, a total of 165 000 forwards–backwards trajectories were calculated for each influence functional. The corresponding CPU time on a Silicon Graphics Origin 200 (with 194 MHz clock cycle and a R10000 processor) is 190 s. At this temperature the high-temperature semiclassical Monte Carlo calculation is essentially exact, and converges with a quite mod-

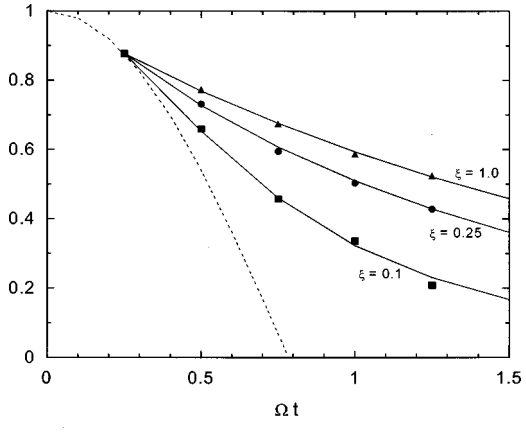

FIG. 2. Average position of a two-level system coupled to a bath of ten harmonic oscillators at a temperature of $\beta^{-1}=20\hbar\Omega$ and three different coupling strengths. The path integral time step is $\Delta t=0.25/\Omega$. Markers: results obtained using the high-temperature semiclassical influence functional formalism. The Monte Carlo error bars are smaller than the markers. Solid line: exact results, generated using the Feynman–Vernon influence functional. Dashed line: dynamics of the bare two-level system.

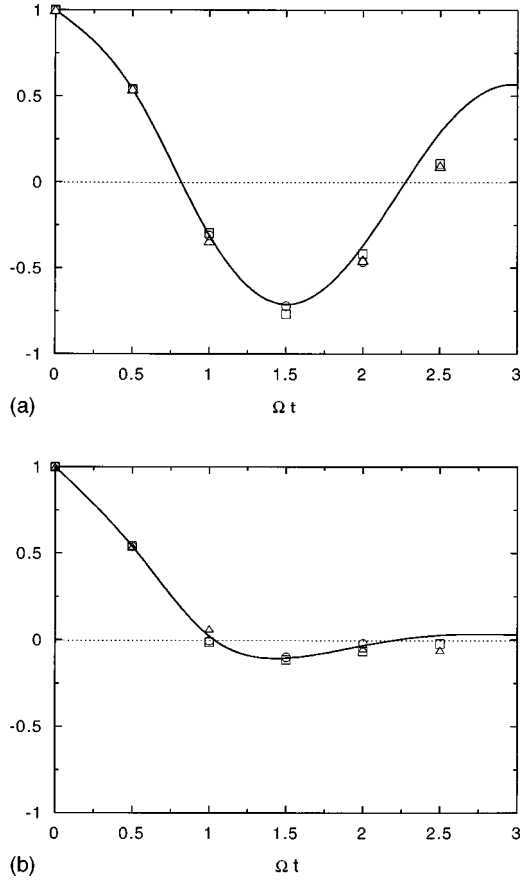

FIG. 3. Average position of a two-level system coupled: (a) weakly ($\xi=0.1$) and (b) moderately strongly ($\xi=0.5$) to a bath of ten harmonic oscillators at a temperature of $\beta^{-1}=\frac{1}{3}\hbar\omega_c$. The path integral time step is $\Delta t=0.5/\Omega$. Markers: results obtained using the imaginary time path integral semiclassical influence functional formalism; triangles: $n=1$; circles: $n=2$; squares: $n=4$. The Monte Carlo error bars are smaller than the markers; solid line: exact results, generated using the Feymman–Vernon influence functional.

TABLE II. Parameters defining anharmonic chain.

Parameter	Value (a.u.)
ϵ	0.9
D_e	1.0
α	1.35
ω	0.008
m	51205
Ω	0.02
c	0.25

est computational effort. It is also worth noting that the path averaging procedure leads to further reduction of the statistical error associated with individual influence functional calculations.

In the low-temperature imaginary time path integral formulation of the semiclassical influence functional ($n>1$), the number of integration variables is considerably larger than in the high-temperature expression. Fortunately, these imaginary time path integral variables enter only as negative real exponents, so there are no more oscillatory terms than before. The increased dimensionality does make the calculation more demanding, although not unfeasible. Figure 3 shows the average position of a two-level system coupled both weakly and quite strongly to the ten-dimensional ohmic bath described above at a temperature equal to $\frac{1}{3}\hbar\omega_c$ for various values of n. At this relatively low temperature the behavior of the TLS ranges from underdamped oscillations at low friction to exponential decay at strong dissipation. It can be seen that at short times the high-temperature approximation ($\hbar\omega_c\Delta\beta=3$) is accurate, but that it breaks down for times greater than about half a period of the system. Convergence of the imaginary time path integral is obtained at this temperature with four ''temperature slices,'' or $\hbar\omega_c\Delta\beta=0.75$ in Eq. (4.13). These calculations were performed with 10 000 Monte Carlo points per integration variable. Note that there are 60 integration variables when four temperature slices are used, so that each influence functional required 600 000 forward–backward trajectories after the initial equilibration. The corresponding CPU time on a Silicon Graphics Origin 200 is approximately 1 h. It is encouraging that the resulting statistical errors are very small and that the qualitatively different dynamics of the two friction regimes considered here are reliably described by the semiclassical influence functional.

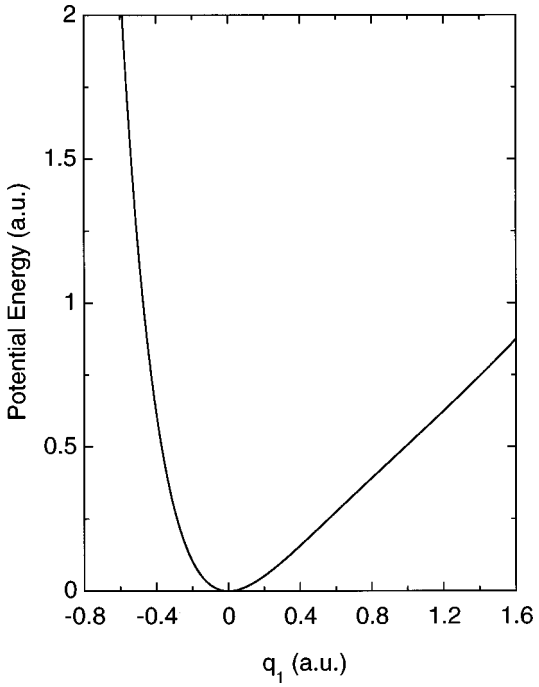

FIG. 4. Anharmonic bath potential energy of Eq. (5.7d) for the case of a single solvent atom.

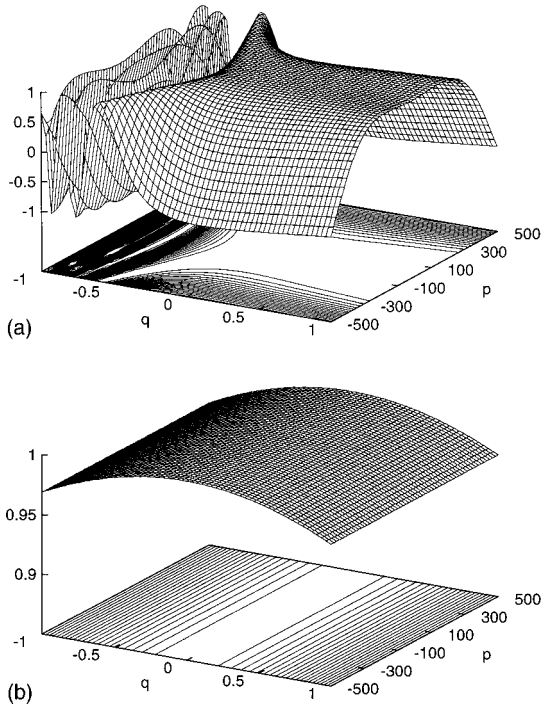

FIG. 5. The real part of the integrand of Eq. (2.20) for the anharmonic potential shown in Fig. 4, as a function of initial position and momentum and an arbitrary pair of system paths. The high temperature approximation, Eq. (3.3), was used to obtain the matrix elements of the Boltzmann operator. (a) the integrand obtained form a path in the conventional forward time direction. (b) The integrand obtained in the present formulation using trajectories which return to zero time.

B. Anharmonic bath

A more stringent test of the proposed methodology is to consider an intrinsically anharmonic, strongly coupled bath. To that end we take a two-level system coupled to a model one-dimensional chain of atoms that can be thought of as modeling various solvation shells. Representing the bath in terms of Cartesian displacement coordinates, the system Hamiltonian is again

$$H_0=-\hbar\Omega\sigma_x. \tag{5.7a}$$

The system-bath coupling is only through the first ''contact'' atom

$$V_{\mathrm{int}}=c\sigma_z q_1, \tag{5.7b}$$

while the bath potential is a sum of pairwise interactions

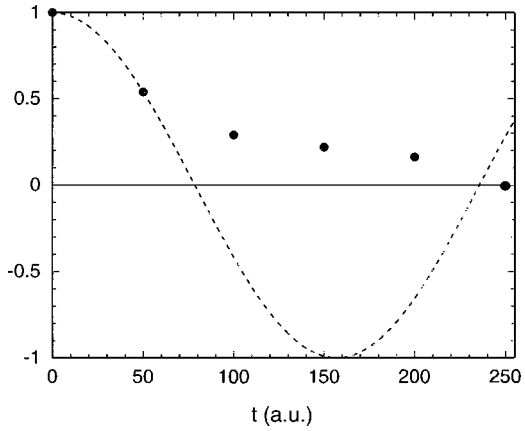

FIG. 6. Average position of the two-level system in Eq. (5.7) coupled to a ten-dimensional strongly anharmonic bath. Markers: results obtained using the high-temperature semiclassical influence functional formalism. The Monte Carlo error bars are smaller than the markers. Dashed line: dynamics of the bare two-level system.

$$V_b(q_1,\ldots,q_n)=V_{\mathrm{sol}}(q_1)+\sum_{k=2}^{n} V_{\mathrm{sol}}(q_k-q_{k-1}), \qquad (5.7c)$$

where

$$V_{\mathrm{sol}}(x)=\varepsilon D_e(1-e^{-\alpha x})^2+(1-\varepsilon)\frac{1}{2}m\omega^2x^2. \qquad (5.7d)$$

The quadratic term in the last equation is added to a Morse potential in order to prevent dissociation, as unbound potentials are difficult to treat with semiclassical propagators. This is not a serious restriction of the method, since such situations are not expected to arise in dense fluids. Table II gives the parameter values (in atomic units) used in this calculation, and Fig. 4 shows V_{sol}, the bath potential for the case of only one solvent atom. Figure 5 shows the integrand of the high-temperature expression for the influence functional for the case of only one solvent atom at select system paths. Note that the highly oscillatory integrand which results from the forwards only propagation shown in Fig. 5(a) is reduced to an extremely smooth function with the forward–backward formulation in Fig. 5(b).

Figure 6 shows the average position of this TLS calculated with the high-temperature formulation of Sec. IV A. The reciprocal temperature is $\beta=100$ a.u. and the path integral time step is 50 a.u. The results were obtained with 10 000 Monte Carlo points per integration variable, such that each influence functional evaluation employed a total of 300 000 trajectories and required 1 h 38 min of CPU time on a Silicon Graphics Origin 200. In this case there are no exact quantum results available for comparison as we are studying the dynamics of a nonlinear system with ten coupled degrees of freedom. Physically, the behavior of the TLS shown in Fig. 6 is reasonable.

VI. CONCLUDING REMARKS

The semiclassical influence functional formalism developed in Ref. 16 and in this article presents a rigorous, yet practical approach to the dynamics of quantum systems in nonlinear many-body environments. The key feature of this approach is evaluation of the forward and backward time propagation in a single step through trajectories that return to zero time, which eliminates the dominant terms from the classical action and leads to smooth propagators that are well suited to numerical integration. At the same time, the interference between the two time evolution operators is fully accounted for, circumventing the need for explicit numerical treatment which would suffer from phase cancellation problems.

The use of a coherent state initial value representation allows a simple phase space sampling. Three procedures are suggested for evaluating the resulting coherent state transform of the Boltzmann operator, including a closed-form high-temperature approximation and a numerical path integral representation. Although the coherent state Boltzmann factor introduces mild oscillations in the integrand, examination of Eqs. (2.14) or (2.18) reveals that in the most important limit where the system forward and backward paths coincide the oscillatory terms cancel exactly and the entire integrand is positive definite. Finally, Monte Carlo schemes were described which employ normalizable sampling functions to generate initial phase space conditions for the classical trajectories.

In the special case of an harmonic oscillator bath, the present formalism yields a semiclassical propagator that is independent of p_0 and which exhibits slow oscillations in q_0, in contrast to the forward-only propagator which is a rapidly oscillatory function of both phase space variables. Although the precise cancellation of the initial momentum is a consequence of linearity in this case, our numerical calculations showed the integrand to exhibit only mild oscillations in the case of an anharmonic bath. We emphasize again that the integrand is *by construction* completely positive in the classical limit of identical system paths for which the influence functional takes on its largest value.

A number of nontrivial test applications were presented in the present article. Application to the model of a harmonic dissipative bath demonstrated that the method converges to the available exact results with modest numerical effort. Further calculations on a multidimensional bath of anharmonically coupled degrees of freedom reminiscent of solvation shells also produced very encouraging results characterized by small error bars. We consider the above models to be representative of many situations involving the dynamics of electron transfer or vibrational relaxation in solution or in polyatomic clusters. Although real chemical applications must be performed to conclusively establish the feasibility of any method, our explorations to date invite considerable optimism in this regard.

ACKNOWLEDGMENTS

This work has been supported by the David and Lucile Packard Foundation through a Packard Fellowship for Science and Engineering. N.M. also acknowledges funding through a National Science Foundation Young Investigator Award, a Sloan Research Fellowship, a Cottrell Scholar Award and a Camille Dreyfus Teacher-Scholar Award.

[1] R. E. Wyatt, Adv. Chem. Phys. **73**, 231-278 (1989).
[2] M. Gruebele and R. Bigwood, Int. Rev. Phys. Chem. **17**, 91 (1998).
[3] E. Galliccio and B. J. Berne, J. Chem. Phys. **101**, 9909 (1994).
[4] E. Galliccio and B. J. Berne, J. Chem. Phys. **105**, 7064 (1996).
[5] N. Makri, Chem. Phys. Lett. **193**, 435 (1992).
[6] C. H. Mak, Phys. Rev. Lett. **68**, 899 (1992).
[7] N. Makri and D. E. Makarov, J. Chem. Phys. **102**, 4611 (1995).
[8] C. H. Mak and R. Egger, Adv. Chem. Phys. **XCIII**, 39 (1996).
[9] J. Cao, L. W. Ungar, and G. A. Voth, J. Chem. Phys. **104**, 4189 (1996).
[10] E. Sim and N. Makri, Comput. Phys. Commun. **99**, 335 (1997).
[11] N. Makri, J. Phys. Chem. **102**, 4414 (1998).
[12] R. B. Gerber, V. Buch, and M. A. Ratner, J. Chem. Phys. **77**, 3022 (1982).
[13] H. Wang, X. Sun, and W. H. Miller, J. Chem. Phys. **108**, 9726 (1998).
[14] A. R. Walton and D. E. Manolopoulos, Mol. Phys. **84**, 961 (1996).
[15] M. L. Brewer, J. S. Hulme, and D. E. Manolopoulos, J. Chem. Phys. **106**, 4832 (1997).
[16] N. Makri and K. Thompson, Chem. Phys. Lett. **291**, 101 (1998).
[17] R. P. Feynman and A. R. Hibbs, *Quantum Mechanics and Path Integrals* (McGraw–Hill, New York, 1965).
[18] R. P. Feynman, *Statistical Mechanics* (Addison-Wesley, Redwood City, 1972).
[19] W. H. Miller, J. Chem. Phys. **53**, 3578 (1970).
[20] W. H. Miller, J. Chem. Phys. **95**, 9428 (1991).
[21] E. J. Heller, J. Chem. Phys. **95**, 9431 (1991).
[22] K. G. Kay, J. Chem. Phys. **100**, 4377 (1994).
[23] M. F. Herman and E. Kluk, Chem. Phys. **91**, 27 (1984).
[24] E. Kluk, M. F. Herman, and H. L. Davis, J. Chem. Phys. **84**, 326 (1986).
[25] A. J. Leggett, S. Chakravarty, A. T. Dorsey, M. P. A. Fisher, A. Garg, and M. Zwerger, Rev. Mod. Phys. **59**, 1 (1987).
[26] N. Makri, J. Phys. Chem. (submitted).
[27] R. P. Feynman and J. F. L. Vernon, Ann. Phys. **24**, 118 (1963).